ORIGINAL PAPER

Randy L. Vander Wal · Gordon M. Berger
Steven D. Mozes

The splash/non-splash boundary upon a dry surface and thin fluid film

Abstract On the basis of empirical data, power-law boundary relations are formulated to delineate the splash and non-splash regions on dry surfaces or thin films under isothermal conditions, using the Ohnesorge and Reynolds numbers. Approximation of the relations permits cancellation of fundamental fluid physical constants to give simplified formulas which provide insight into the governing parameters describing splashing and non-splashing behaviors. Thus, for a droplet impinging upon a dry solid surface, the splash/non-splash border is well described by $\sqrt{Ca} = 0.35$. For a drop impinging upon a thin fluid film, the analytical simplification yields a boundary described by $\sqrt{We} = 20$. For both expressions, values greater than the numerical value result in splashing.

1 Introduction

It is essential to understand the underlying mechanisms governing the impact and spread of liquid droplets upon a solid surface in many processes such as ink-jet printing, painting, pesticide spraying and spray cooling. Each application will benefit from a specific result. The situation is further complicated because many modes of splashing can occur, ranging from splash on impact to prompt splash upon spreading, delayed splash or crown breakup, partial rebound and jetting. Across this range of splashing behaviors, the success of each of these applications will depend on controlling splashing behavior. Given the exceeding complexity of an impact event, simple interpretations for the droplet–surface interaction based on fluid parameters are sought.

While the dependence upon the fluid parameters can provide insights into the splashing mechanism, a predictive correlation, even if empirically based, would be useful for gauging splash probabilities and designing systems or tailoring conditions so as to achieve vigorous splashing or avoiding splashing altogether.

Towards this goal, various investigators have sought to delineate the boundary between splashing and non-splashing regions based on various relationships between non-dimensional parameters.

For example, Stow and Hadfield (1981) found a correlation for the splashing/deposition limit, which is expressed as, $Re^{0.31} We^{0.69} = \xi$—where Re is the Reynolds number, We is the Weber number and ξ is the splash deposition value. Notably, it is dependent upon the surface roughness. Wu (1992) later simplified the Stow and Hadfield formula for small values of Ohnesorge (Oh) number, where the influence of viscosity was minimal. Mundo et al. (1995) investigated the splashing/deposition limit using a combination of Oh and Re numbers. Their correlation is expressed as $Oh\, Re^{1.25} = 57.7$. They also included relations for the splashed droplet mean size and deposited mass fraction. A distinct correlation between the Re and Oh number was found only if the normal velocity component of the impinging droplets was used in their calculation. Though Mundo et al. (1995) found no difference for two values of surface roughness, Cossali et al. (1997) later pointed out that Mundo et al.'s (1995) values of surface roughness were in an asymptotic regime where the ξ parameter of Stow and Hadfield achieved a nearly constant value. Consequently, although there appears to be some consistency, the formulas presented above are largely unverified as Stow and Hadfield used only water while Mundo et al. (1995) investigated a range of fluid properties using a rotating surface, which imparts a translational vector to the drop impingement dynamics.

R. L. V. Wal (✉) · G. M. Berger · S. D. Mozes
NASA-Glenn, M.S. 110-3, 21000 Brookpark Road,
Cleveland, OH, 44135 USA
E-mail: randy@rvander.grc.nasa.gov
Tel.: +1-216-4339065
Fax: +1-216-4333793

The situation is further complicated by different kinds of splashes ranging from prompt, crown break-up, receding breakup and partial rebounds, all of which have been observed to depend upon other variables. Therein, an alternative approach has been identified to develop empirical correlations in which the range of outcomes is mapped against the test conditions. Thereby, specific impact outcomes or impact regime "maps" have been developed as a function of droplet velocity, surface temperature, impact angle, surface curvature and roughness (Wachters and Westerling 1966; Stow and Hadfield 1981; Ko and Chung 1996; Mundo et al. 1995; Bernadin et al. 1997; Cossali et al. 1997; Range and Feuillebois 1998; Hardalupas et al. 1999; Crooks and Boger 2000; Kang and Lee 2000; Karl et al., 2000; Lavergne and Platet 2000; Wu 2003). Yet other works have characterized droplet rebound, partial and intact, as a function of fluid properties, surface wettability and impact energy (Hobbs and Kezweeny 1966; Akao et al. 1980; Shi and Chen 1983; Chandra and Avedesian 1991; Fukai et al. 1995; Hatta et al. 1995; Scheller and Bousfield 1995; Pasandideh-Fard et al. 1996; Zhao et al. 1996; Mao et al. 1997; Mourougou-Candoni et al. 1997; Zhang and Basaran 1997; Prunet-Foch et al. 1998; Thoroddsen and Sakakibara 1998; Mourougou-Candoni et al. 1999; Roisman et al. 1999; Rioboo et al. 2001; Rioboo et al. 2002; Rozhkov et al. 2002; Yang and Leong 2002; Kim et al. 2003). Notably, neither the power-law relations nor the empirical correlations provide an explanation for the splashing mechanism. This is not particularly surprising given the variety of splashing modes that can occur, depending upon fluid physical properties and impact conditions (Rein 1996; Rioboo et al. 2001; Rioboo et al. 2002).

Although several studies have been performed on drops impacting upon deep pools (Engel 1967; Levin and Hobbs 1971; Cai 1989; Oguz and Prosperetti 1989; Pumphrey and Elmore 1990; Shin and McMahon 1990; Peck and Sigurdson 1994; Cresswell and Morton 1995; Thoroddsen and Takehara 2000; Kersten et al. 2003), fewer have used thin fluid films (Yarin and Weiss 1995; Cossali et al. 1997; Coghe et al. 1999; Wang and Chen 2000; Sivakumar and Tropea 2002; Rioboo et al. 2003). Some of these latter studies have provided detailed characterization of the secondary droplets number, size and velocity for some selected fluids (Hobbs and Osheroff 1967; Stow and Stainer 1977; Mundo et al. 1995; Cossali et al. 1997; Cossali et al. 1999). Among these studies, only four appear to have investigated a splash threshold as has been done for impact upon dry solid surfaces (Yarin and Weiss 1995; Cossali et al. 1997; Wang and Chen 2000; Rioboo et al. 2003). This is particularly surprising as many applications will quickly transform into one where subsequent drops impact upon a liquid film formed by previous drops. Moreover, these numerical relations or empirical graphical boundaries do not provide insight into the mechanism(s) or fluid parameters governing splashing.

Given an incomplete understanding of drop splashing, in this article we investigate the splash/non-splash boundary for drops impacting upon a dry surface and one wetted by a thin film, for isothermal systems. In spray or paint applications, a thin film represents the first transition from a dry surface towards thicker fluid layers. Moreover, thin films present the largest contrast with a dry surface and initiate splashing before intermediate or thick fluid films. Here, the usage of a mirrored surface permitted focus upon the fluid properties, while effects of surface roughness are addressed in a companion paper. To encompass a broad range of fluid properties, the splashing onsets of 12 fluids with $20.1 < \sigma < 72.8$ and $0.409 < \mu < 3.34$, where σ and μ are respectively the surface tension and viscosity, were found. Within this range of impact conditions and fluid properties, empirical relations delineating the boundary between splash and non-splash regions of behavior were determined using the Oh and Re numbers. To lend insight into the physical parameters governing the onset of splashing, algebraic simplification of the power-law relations was performed to shed light on the underlying splashing mechanism and to illuminate the competing effects of viscosity and surface tension upon impact outcome. For practical reasons, all splash modes occurring in close proximity to impact are included here, which excludes all rebound-based jetting.

2 Experimental

The setup includes an impact platform that holds a dry diamond-lathed aluminum disk, with mean surface roughness less than 10 nm, or a thin pool of approximately 0.02 cm of a desired fluid over a similar aluminum disk. The film thickness was measured using an indenter, a needle mounted on a vertical micro-translation stage to measure the distance from the top of the liquid layer to the submerged metal insert, aided by the free-running camera system.

The inertial-based release mechanism includes interchangeable needles to hold different volumes of a wide variety of liquids with many different physical properties. Droplets were measured with a microsyringe and manually placed on the needle. A droplet of 0.20 cm diameter (4.0 μL) was chosen because the liquid maintained a spherical shape throughout the free fall, negating concerns of an uneven impact. The liquid was deployed by way of a manual trigger that released a stretched rubber band at the top of the mechanism. The relaxing rubber band then pulled the needle quickly upward, moving it out of the liquid droplet and allowing the droplet to fall onto the film below.

A Kodak EktaPro HG 2000 high-speed camera was then manually triggered and it recorded the droplet impact at 2,000 frames/s for half of the imaging field. The exposure time was set at 28 μs while using a 105-mm Nikkor lens set at an aperture of 32 to minimize motion

blurring and to provide a large depth of field. A halogen lamp illuminated the impact site through a single sheet of Roscoe 111 diffusion film to provide uniform high-intensity back lighting.

Droplet velocities were increased or decreased by translating the release mechanism vertically and taking advantage of gravitational acceleration. All velocities were measured using XCAP 2.0, an image acquisition and analysis program from EPIX. Measured velocities have an error of ± 0.15 m/s based on the pixel size and 0.5 ms image spacing.

The fluids used include alkanes and alcohols, whose properties were gathered experimentally or through the *CRC Handbook of Chemistry and Physics* (Weast 1973). Water and the 30 wt% glycerol–water solution were also used. Deionized water was obtained from a Millipore AFS filtration system. The properties of the glycerol solution were measured using a Cannon-Fenske (Reverse Flow) viscometer and Cahn tensiometer. As a consequence of the native oxide layer that formed upon the surface, hydrocarbon fluids fully wetted the surface while water, water–glycerol and alcohols had a contact angle near 30°. Table 1 contains the relevant properties of the fluids used in this study.

To verify the results for any given set of impact conditions, generally three separate tests were conducted. The record of outcomes was binary in nature; either splashing or no splashing was observed. Detailed pictures defining splashing behavior more broadly may be found in a companion paper.

For reference, the Weber number is given by

$$We = \frac{\rho v^2 d}{\sigma} \quad (1)$$

while the Reynolds number is given by

$$Re = \frac{\rho v d}{\mu} \quad (2)$$

with the Ohnesorge number expressed as

$$Oh = \frac{\sqrt{We}}{Re} \quad (3)$$

Finally, the Capillary number (Ca) is

$$Ca = \frac{\mu v}{\sigma} \quad (4)$$

where ρ is the fluid density, d is the droplet diameter, v the droplet impact velocity, σ the fluid surface tension and μ is the fluid viscosity.

3 Results

To illustrate the range of non-dimensional parameters and their dependence upon fluid physical parameters, the data summarized in Tables 2, 3, 4 are organized in columns by increasing velocity at which the droplet approaches the surface. Correspondingly, the Re, We and Ca numbers will increase with the velocity and fluid order.

The *shaded cells* illustrate the values for the particular fluid that splash upon a dry surface. As Tables 2 and 3 illustrate, the boundary for splashing is not uniformly monotonic with either Re or We number; discontinuities are evident. Considered individually, neither scaled kinetic energy, as expressed by the We number, nor scaled momentum, as represented by the Re number, consistently defines a clear boundary between splashing and non-splashing. Therein, it is not surprising that the correlations developed to date are based on both We and Re numbers to encompass more degrees of freedom by including both fluid viscosity and surface tension.

This lack of simple correlative data using individual non-dimensional parameters serves as a motivation for the development of an algebraic relation based on combinations of these parameters to describe the splashing/non-splashing boundary. The data for the splashing and non-splashing impact conditions upon a dry, solid surface are plotted in Fig. 1. Each symbol shape corresponds to a particular fluid, as indicated in the legend. The red data points correspond to splashing drops while the blue points correspond to impacting

Table 1 Key physical properties of the fluids used

Fluid	Viscosity (centipoise)	Surface tension (dynes/cm)	Density (g/cm^3)
Heptane	0.409	20.1	0.684
Nonane	0.711	22.9	0.722
Decane	0.925	24.0	0.730
Dodecane	1.35	25.4	0.750
Tetradecane	2.04	26.7	0.763
Hexadecane	3.34	27.1	0.773
DI water	0.978	72.8	1.00
30% glycerol/water	2.64	71.7	1.08
Methanol	0.597	22.6	0.792
Ethanol	1.20	23.1	0.789
N-propanol	2.26	23.8	0.804
Butanol	2.95	20.1	0.810

Table 2 Reynolds numbers achieved at a range of impact velocities

Reynolds	Impact velocity on a dry surface			
Fluid	2.17 m/s	3.15 m/s	3.80 m/s	4.22 m/s
Hexadecane	*988*	*1,440*	*1,730*	*1,930*
Butanol	*1,170*	*1,710*	*2,060*	*2,290*
N-propanol	*1,520*	*2,210*	*2,670*	*2,960*
Tetradecane	*1,600*	*2,320*	*2,800*	*3,110*
30% glycerol/water	1,740	2,530	*3,060*	*3,400*
Dodecane	2,370	*3,450*	*4,160*	*4,620*
Ethanol	2,810	*4,080*	*4,920*	*5,470*
Decane	3,370	*4,900*	*5,910*	*6,570*
Nonane	4,330	6,300	7,600	8,450
DI water	4,370	6,350	7,650	8,510
Methanol	5,660	8,230	9,930	11,000
Heptane	7,140	10,400	12,500	13,900

Splashing events on a dry surface are italicized

Table 3 Weber numbers achieved at a range of impact velocities

Weber	Impact velocity on a dry surface			
Fluid	2.17 m/s	3.15 m/s	3.80 m/s	4.22 m/s
DI water	127	269	391	483
30% glycerol/water	139	294	*427*	*528*
Tetradecane	*264*	*559*	*813*	*1,000*
Hexadecane	*265*	*559*	*813*	*1,000*
Dodecane	273	578	840	1,040
Decane	282	595	865	1,070
Nonane	292	616	896	1,110
N-Propanol	*313*	*661*	*961*	*1,190*
Heptane	315	665	967	1,200
Ethanol	317	*670*	*974*	*1,200*
Methanol	324	685	996	1,231
Butanol	*373*	*788*	*1,150*	*1,420*

Splashing events on a dry surface are italicized

Table 4 Capillary numbers achieved at a range of impact velocities

| Capillary	Impact velocity on a dry surface			
Fluid	2.17 m/s	3.15 m/s	3.80 m/s	4.22 m/s
DI water	2.91	4.23	5.10	5.67
Heptane	4.41	6.41	7.73	8.60
Methanol	5.72	8.32	10.0	11.2
Nonane	6.73	9.78	11.8	13.1
30% glycerol/water	7.98	11.6	*14.0*	*15.6*
Decane	8.36	*12.2*	*14.7*	*16.3*
Ethanol	11.3	16.4	*19.8*	*22.0*
Dodecane	11.5	*16.8*	*20.2*	*22.5*
Tetradecane	*16.6*	*24.1*	*29.0*	*32.3*
N-propanol	*20.6*	*29.9*	*36.1*	*40.1*
Hexadecane	*26.8*	*38.9*	*46.9*	*52.2*
Butanol	*31.8*	*46.2*	*55.7*	*62.0*

Splashing events on a dry surface are italicized

drops for which no splash occurred. Several combinations of Oh, Re, We and Froude numbers were tested to summarize the splash/non-splash data for droplets impacting upon the dry surface and the thin film. Only the power-law correlation based on the Oh and Re numbers proved fruitful in defining a clear boundary between these behavior regimes. The dashed curved line represents an empirical splashing boundary for the fluids studied here and is described by the relation

$$Oh \times Re^{0.609} = 0.85 \qquad (5)$$

Values greater than the numerical value result in splashing. The occurrence of splashing was observed as a
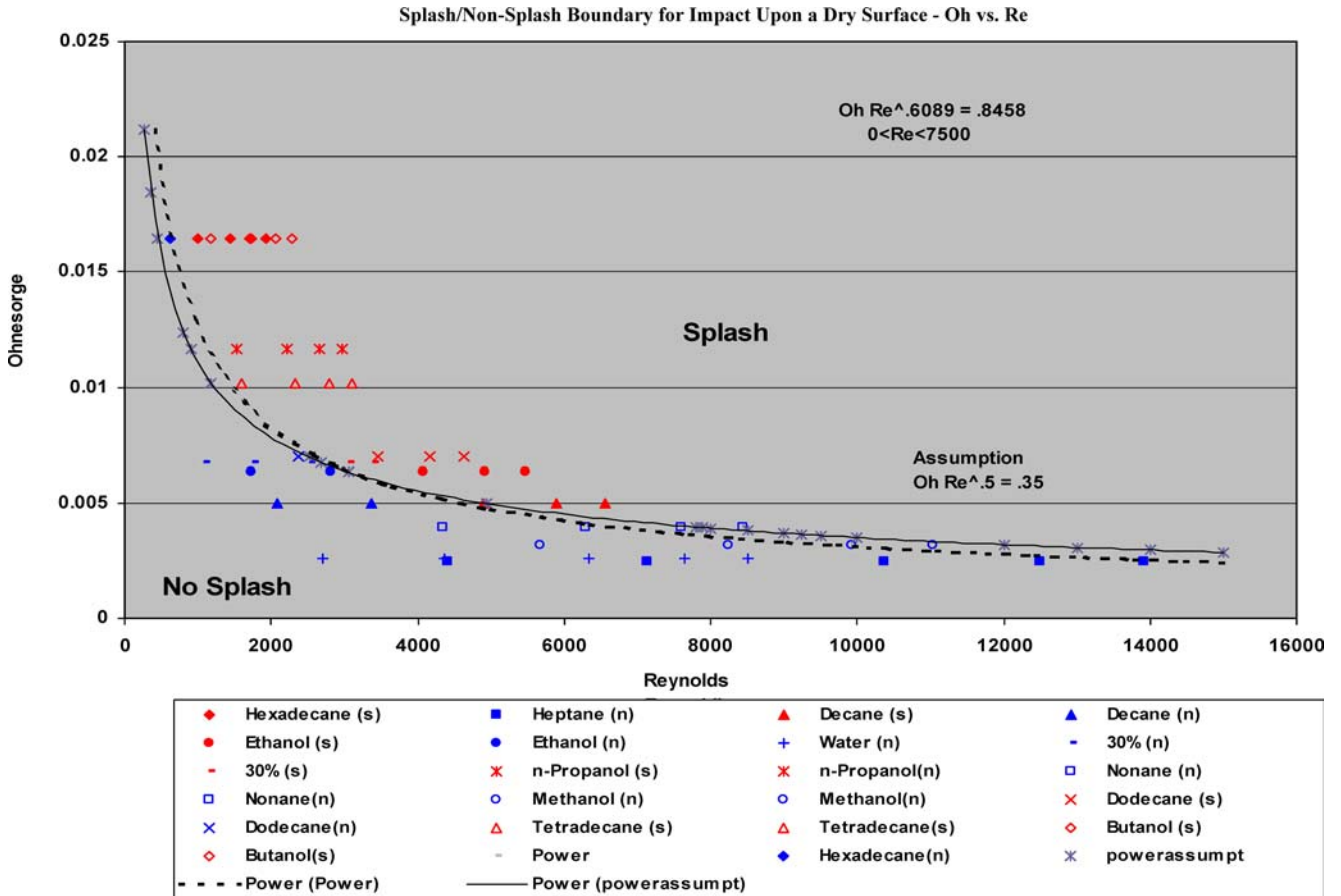
Fig. 1 Splash behavior on a dry surface plotted with respect to Ohnesorge and Reynolds number values. *Red plot* marks correspond to splashing behavior and *blue* to non-splash. The equation for the boundary fit line is included on the graph, in addition to using the simplified form
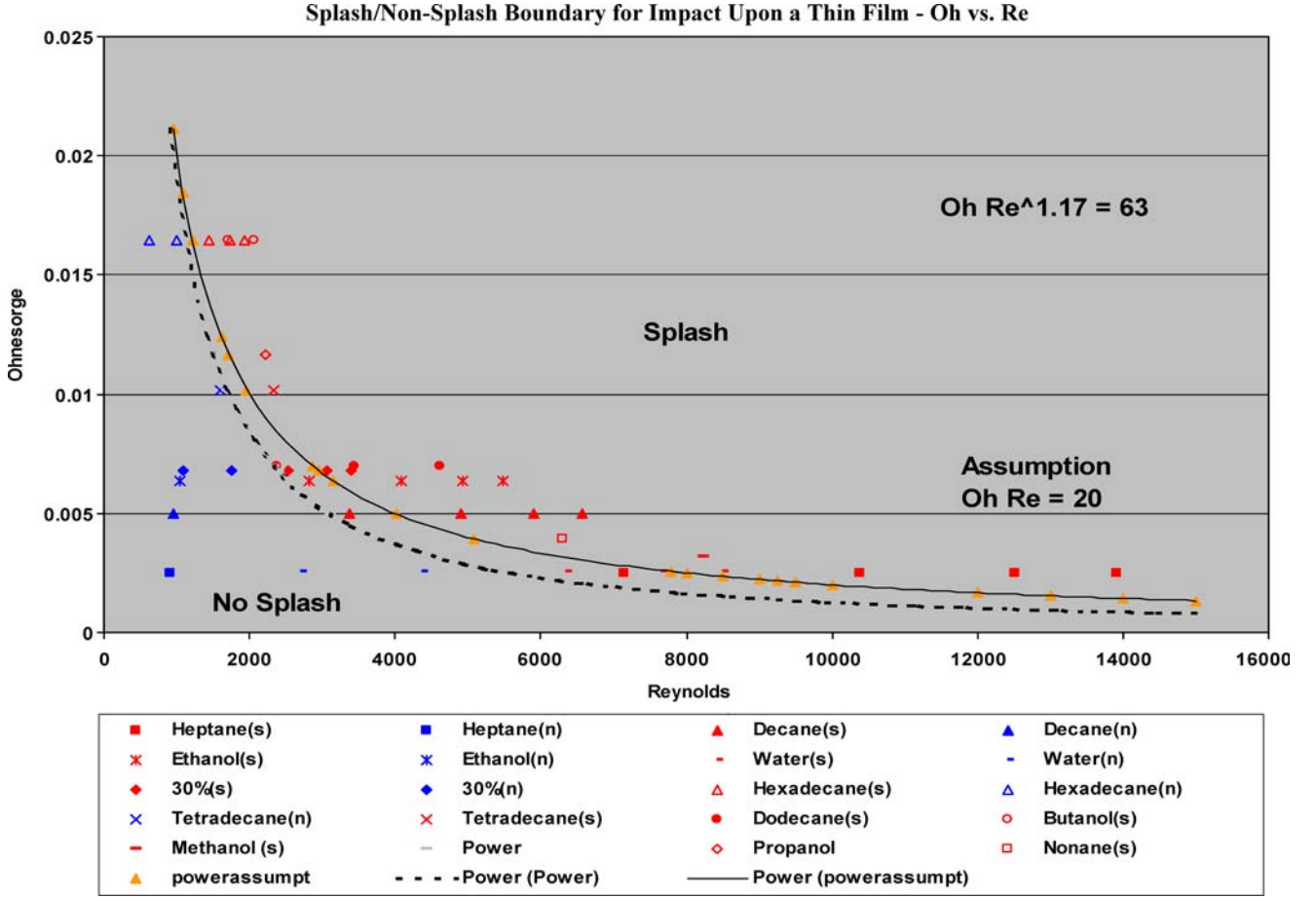
Fig. 2 Splash behavior on a thin film plotted with respect to Ohnesorge and Reynolds number values. *Red plot* marks correspond to splashing behavior and *blue* to non-splash. The equation for the boundary fit line is included on the graph, in addition to using the simplified form

radial jetting of fluid during droplet spreading. The range of surface tensions and viscosities represented by this map generates a wide predictive capability. The particular appeal of using the Oh number is that it contains a dependence upon both surface tension and viscosity. Recognition of the definitions of Oh and Re in terms of fundamental fluid physical parameters and making the approximation that $Re^{0.609} = Re^{0.5}$ permit algebraic simplification. Thus equation 5 may be rewritten as

$$Oh\sqrt{Re} = \frac{\mu}{\sqrt{\rho\sigma d}} \times \frac{\sqrt{\rho v d}}{\mu} = \frac{\sqrt{\mu v}}{\sqrt{\sigma}} = \sqrt{Ca} \qquad (6)$$

This relation is also plotted in Fig. 1 as the solid curve. The numerical value of the constant, as may be found in Fig. 1, was readjusted as necessary to produce the best delineation between the splash and non-splashing events. As expected, both viscosity and surface tension are involved. Notably, the splash/non-splash boundary has an opposite dependence upon each parameter. High surface tension acts to restrict splashing as fluid extension increases surface area and hence energy. Conversely, high viscosity acts to promote splashing. This is

consistent with the origin of splashing being a kinematic discontinuity and ensuing instability phenomena within the outward directed fluid (Allen 1975; Yarin and Weiss 1995; Rieber and Frohn 1999; Bussman et al. 2000; Kim et al. 2000; Trujillo and Lee 2001; Roisman and Tropea, 2002; Josserand and Zaleski 2003). High viscosity acts to retard the initial edge of the outward flowing fluid more than latter portions, thereby creating a velocity discontinuity that results in splashing. This relationship is further supported by the splash/non-splash occurrence at a range of Ca numbers recorded in Table 4.

The presence of a thin film causes a dramatic shift in the splashing threshold for all of the fluids studied here. Significantly, differences between the thresholds for the fluids largely disappear. Figure 2 shows a plot summarizing the splash and non-splash data for drops impacting upon a thin fluid film covering a dry solid surface. The splash/non-splash symbolism is the same as before. Significantly, the boundary delineating the splash and non-splash regions also follows a power-law relation in terms of Oh and Re as given by,

$$Oh \times Re^{1.17} = 63 \qquad (7)$$

Values greater than the numerical value result in splashing. Upon the thin film, splashing was manifested as droplets breaking off of the developing crown and of the receding crown. Using the definitions of the non-dimensional parameters in terms of the fundamental fluid physical properties as before and approximating $Re^{1.17} = Re$ permit algebraic cancellation of like terms to yield,

$$\text{Oh Re} = \frac{\mu}{\sqrt{\rho\sigma d}} \times \frac{\rho\sigma d}{\mu} = \frac{v\sqrt{\rho d}}{\sqrt{\sigma}} = \sqrt{\text{We}} \qquad (8)$$

This relation is also plotted in Fig. 2 as the solid curve. The numerical value of the constant, as may be found in Fig. 2, was readjusted as necessary to produce the best delineation between the splash and non-splashing events. For a drop impacting upon a thin fluid film, splashing was observed to occur at far lower We numbers than for a dry surface. In light of the kinematic discontinuity model, this is to be expected. The fluid within the thin film is initially stationary; hence, there exists a very large velocity discontinuity between the outwardly directed droplet fluid and the initially stationary fluid of the thin film. This is undoubtedly larger than velocity differences within the droplet fluid that arise during different stages of the drop impact and deformation. Hence, the presence of the static fluid of the film governs the splashing threshold while the fluid viscosity is relegated to a secondary role in the splash dynamics. This is reflected by the absence of fluid viscosity in Eq. 8 and is consistent with past observations and numerical calculations (Vander Wal et al. 2005).

It should be noted that expressions 6 and 8 are only approximations; in particular, the thin film expression misses a few splashing instances. However, the approximations allow simple physical insights to be gained. Strictly speaking, as seen from Eq. 5 and 6 prior to simplification, the boundary for splashing upon a dry surface will have a weak dependence upon the initial drop diameter. Correspondingly, the splash/non-splash boundary for a drop impacting upon a thin film will have a weak dependence upon the droplet fluid viscosity. As both expressions involve the creation of a kinematic discontinuity within the expanding fluid film, it is not surprising that each simplified expression depends upon the drop velocity. For impact upon the film, the dependence upon velocity is stronger, mirroring the observation that splashing occurs at much lower We number values than for impact upon a dry surface for any given fluid.

4 Conclusions

Determining the splash/non-splash boundary is important for many practical applications. Painting, coating and cooling processes would each benefit from near-term empirical relations and subsequent models. Such demarcations can guide theoretical development by providing definitive testing of its predictive capabilities. Thus, empirical relations describing the boundary between splash and non-splash were given for drops impinging upon a dry solid surface and upon a thin fluid film covering a similar surface. Analytical simplification of the power laws describing the boundary between the splash and non-splash regions yields insight into the fundamental physical properties governing the splash and non-splash outcomes of the fluid droplets. Therein, splashing upon a dry surface is reasonably described by $\sqrt{Ca} > 0.35$, reflecting the competing roles of surface tension and viscosity. Splashing upon a thin fluid film, as described by $\sqrt{We} > 20$, is governed by fluid density and surface tension, but is rather independent of viscosity. Finally, the data presented here suggests that a more direct dependence upon the surface tension and viscosity, given a better understanding of their interplay, would allow parallel relations to be developed for droplet-surface impacts of more complicated situations involving non-Newtonian fluids, specifically those exhibiting viscoelastic behavior.

5 Disclaimer

Trade names or manufacturers' names are used for identification only. This usage does not constitute an official endorsement, either expressed or implied by either the National Aeronautics and Space Administration or The National Center for Microgravity Research.

References

Akao F, Araki K, Mori S, Moriyama A (1980) Deformation behavior of a liquid droplet impinging onto hot metal surface. Trans Iron Steel Inst Jpn 20:737–743

Allen RF (1975) The role of surface tension in splashing. J Colloid Surf Sci 51:350–351

Bernardin JD, Stebbins CJ, Mudawar I (1997) Mapping of impact and heat transfer regimes of water drops impinging on a polished surface. Int J Heat Mass Transfer 40:247–267

Bussman M, Chandra S, Mostaghimi J (2000) Modeling the splash of a droplet impacting a solid surface. Phys Fluids 12:3121–3132

Cai YK (1989) Phenomena of a liquid drop falling to a liquid surface. Exp Fluids 7:388–394

Chandra S, Avedisian CT (1991) On the collision of a droplet with a solid surface. Proc R Soc London Ser A 432:13

Coghe A, Brunello G, Cossali GE Marengo M (1999) Single drop splash on thin film: measurements of crown characteristics. In: ILASS Europe 1999

Cossali GE, Coghe A, Marengo M (1997) The impact of a single drop on a wetted solid surface. Exp Fluids 22:463–472

Cossali GE, Brunello G, Coghe A, Marengo M (1999) Impact of a single drop on a liquid film: Experimental analysis and com-

parison with empirical models. In: Italian congress of thermo-fluid dynamics UIT, Ferrara, 30th June–2nd June 1999

Cresswell RW, Morton BR (1995) Drop-formed vortex rings: the generation of vorticity. Phys Fluids 7:1363–1370

Crooks R, Boger DV (2000) Influence of fluid elasticity on drops impacting on dry surfaces. J Rheol 4:973–996

Engel OG (1967) Initial pressure, initial flow velocity and the time dependence of crater depth in fluid impacts. J Appl Phys 38:3935–3940

Fukai J, Shiiba Y, Yamamoto T, Miyatake O, Poulikakos D, Megaridis CM, Zhao Z (1995) Wetting effects on the spreading of a liquid droplet colliding with a flat surface: experiment and modeling. Phys Fluids 7:236–247

Hardalupas Y, Taylor AMKP, Wilkins JH (1999) Experimental investigation of sub-millimeter droplet impingement onto spherical surfaces. Int J Heat Fluid Flow 20:477–485

Hatta N, Fujimoto H, Takuda H (1995) Deformation process of a water droplet impinging on a solid surface. J Heat Transfer 117:394–401

Hobbs PV, Kezweeny AJ (1966) Splashing of a water drop. Science 155:1112–1114

Hobbs PV, Osheroff T (1967) Splashing of drops on shallow liquids. Science 158:1184–1186

Josserand C, Zaleski S (2003) Droplet splashing on a thin liquid film. Phys Fluids 15:1650–1657

Kang BS, Lee DH (2000) On the dynamic behavior of a liquid droplet impacting upon an inclined heated surface. Exp Fluids 29:380–387

Karl A, Frohn A (2000) Experimental investigation of interaction processes between droplets and hot walls. Phys Fluids 12:785–796

Kersten B, Ohl CD, Prosperetti A (2003) Transient impact of a liquid column on a miscible liquid surface. Phys Fluids 15:821–824

Kim H-Y, Feng ZC, Chun J-H (2000) Instability of a liquid jet emerging from a droplet upon collision with a solid surface. Phys Fluids 12:531–541

Kim H-Y, Park S-Y, and Min K (2003) Imaging the high-speed impact of microdrop on solid surface. Rev Sci Instrum 74:4930–4937

Ko YS, Chung SH (1996) An experiment on the breakup of impinging droplets on a hot surface. Exp Fluids 21:118–123

Lavergne G, Platet B (2000) Droplet impingement on cold and wet wall. In: ILASS-Europe, VII:12.1–12.7, 11–13 September 2000

Levin Z, Hobbs PV (1971) Splashing of water drops on solid and wetted surfaces: hydrodynamics and charge separation. Philos Trans R Soc Lond Ser A 269:555

Mao TM, Kuhn DCS, Tran H (1997) Spread and rebound of liquid droplets upon impact on flat surfaces. AIChE J 43:2169–2179

Mourougou-Candoni N, Prunet-Foch B, Legay F, Vignes-Adler M, Wong K (1997) Influence of dynamic surface tension on the spreading of surfactant solution droplets impacting onto a low-surface energy solid substrate. J Colloid Interface Sci 192:129–141

Mourougou-Candoni N, Prunet-Foch B, Legay F, Vignes-Adler M (1999) Retraction phenomena of surfactant solution drops upon impact on a solid substrate of low surface energy. Langmuir 15:6563–6574

Mundo CHR, Sommerfeld M, Tropea C (1995) Droplet-wall collisions: experimental studies of the deformation and breakup process. Int J Multiphase Flow 21:151–173

Oguz HN, Prosperetti A (1989) Surface tension effects in the contact of liquid surfaces. J Fluid Mech 203:149–171

Pasandideh-Fard M, Qiao YM, Chandra S, Mostaghimi J (1996) Capillary effects during droplet impact on a solid surface. Phys Fluids 8:650–659

Peck B, Sigurdson L (1994) The three dimensional vortex structure of an impacting water drop. Phys Fluids 6:564–576

Prunet-Foch B, Legay F, Vignes-Adler M, Delmotte C (1998) Impacting emulsion drop on a steel plate: influence of the solid substrate. J Colloid Interface Sci 199:151–168

Pumphrey HC, Elmore PA (1990) The entrainment of bubbles by drop impacts. J Fluid Mech 220:539–567

Range K, Feuillebois F (1998) Influence of surface roughness on liquid drop impact. J Coll Int Sci 203:16–30

Rein M (1996) The translational regime between coalescing and splashing drops. J Fluid Mech 306:145–165

Rieber M, Frohn A (1999) A numerical study on the mechanism of splashing. Int J Heat Fluid Flow 20:455–461

Rioboo R, Tropea C, Marengo M (2001) Outcomes from a drop impact on solid surfaces. Atomization Sprays 11:155–165

Rioboo R, Marengo M, Tropea C (2002) Time evolution of liquid drop impact onto solid dry surfaces. Exp Fluids 33:112–124

Rioboo R, Bauthier C, Conti J, Voue M, De Connick J (2003) Experimental investigation of splash and crown formation during single drop impact upon wetted surfaces. Exp Fluids 32:1–8

Roisman IV, Tropea C (2002) Impact of a drop onto a wetted wall: description of crown formation and propagation. J Fluid Mech 472:373–397

Roisman IV, Araneo L, Marengo M, Tropea C (1999) Evaluation of drop impingement models: experimental and numerical analysis of a spray impact. In: ILASS-Europe'99, Toulouse, France

Rozhkov A, Prunet-Foch B, Vignes-Adler M (2002) Impact of water drops on small targets. Phys Fluids 14:3485–3501

Scheller BL, Bousfield DW (1995) Newtonian drop impact with a solid surface. AIChE J 41:1357–1367

Shi MH, Chen JC (1983) Behavior of a liquid droplet impinging on a solid surface. ASME 83-Wa/HT-104

Shin J, McMahon TA (1990) The tuning of a splash. Phys Fluids A2:1312–1317

Sivakumar D, Tropea C (2002) Splashing impact of a spray onto a liquid film. Phys Fluids 14:L85–L88

Stow CD, Hadfield MG (1981) An experimental investigation of fluid flow resulting from the impact of a water drop with an unyielding dry surface. Proc R Soc Lond A 373:419–441

Stow CD, Stainer RD (1977) The physical products of a splashing water drop. J Meterol Soc Jpn 55:518–531

Thoroddsen ST, Sakakibara J (1998) Evolution of the fingering pattern of an impacting drop. Phys Fluids 10:1359–1374

Thoroddsen ST, Takehara K (2000) The coalescence cascade of a drop. Phys Fluids 12:1265–1267

Trujillo MF, Lee CF (2001) Modeling crown formation due to the splashing of a droplet. Phys Fluids 13:2503–2516

Vander Wal RL, Berger GM, Mozes SD (2005) Droplets splashing upon films of the same fluid of various depths

Wang A-B, Chen C-C (2000) Splashing impact of a single drop onto very thin liquid films. Phys Fluids 12:2155–2158

Weast RC (ed) (1973) Chemical rubber company handbook of chemistry and physics, 54th edn. Cleveland

Wu Z-N (1992) Modelisation et calcul implicite multidomaine d'ecoulements diphasiques gaz-gouttelettes. PhD Thesis, Universite Pierre et Marie Curie

Wu Z-N (2003) Approximate critical Weber number for the breakup of an expanding torus. Acta Mech 0:1–9

Yang C, Leong KC (2002) Influences of substrate wettability and liquid viscosity on isothermal spreading of liquid droplets on solid surfaces. Exp Fluids 33:728–731

Yarin AL, Weiss D (1995) Impact of drops on solid surface: self-similar capillary waves and splashing as a new type of cinematic discontinuity. J Fluid Mech 283:141–173

Zhang X, Basaran OA (1997) Dynamic surface tension effects in impact of a drop with a solid surface. J Colloid Interface Sci 187:166–178

Zhao Z, Poulikakos D, Fukai J (1996) Heat transfer and fluid dynamics during the collision of a liquid droplet on a substrate-II. Modeling. Int J Heat Mass Transfer 39:2791–2802